

New and Primary production in the western Indian Ocean during Fall monsoon

V.V.S.S. Sarma* and H.B. Dalabehera

CSIR-National Institute of Oceanography,
Regional Centre, 176 Lawsons Bay Colony,
Visakhapatnam, India

*Corresponding author (sarmav@nio.org)

Abstract

To examine the spatial variability and controlling factors of new, regenerated and primary productions, 21 stations were studied during fall monsoon period in the western Indian Ocean under Indian-GEOTRACES program. The primary, new and regenerated productions were estimated based on the incubation of enriched $^{13}\text{C}_{\text{HCO}_3}$ and $^{15}\text{N}_{\text{NO}_3}$, $^{15}\text{N}_{\text{NH}_4}$ tracers respectively. High nitrate and phosphate concentrations were observed in the upper 30 m of water column in the Arabian Sea (AS) due to advection of upwelled waters from Oman and Somalia coasts. Chl-*a* in the upper 25 m of water column was low with prominent subsurface Chl-*a* maximum ($0.5\text{-}1.3\text{ mg m}^{-3}$) between 25 and 50 m. The mean new production was almost similar in the AS and the South Indian Ocean (SIO; north of 30°S) with higher regenerated production in the SIO than AS. The photic zone integrated nitrate, and phosphate showed positive relation with primary production and negative relation with new and regenerated production. The photic zone integrated primary production was more than double in the AS ($1238\pm 626\text{ mg C m}^{-2}\text{ d}^{-1}$) compared to the SIO ($675\pm 431\text{ mg C m}^{-2}\text{ d}^{-1}$) with significant positive relation with photic zone integrated Chl-*a*. The range of primary production observed in the Indian Ocean ($236\text{-}1899\text{ mgC m}^{-2}\text{ d}^{-1}$) is within the range observed in the tropical Pacific and Atlantic Oceans ($210\text{-}1887\text{ mgC m}^{-2}\text{ d}^{-1}$). The contribution of primary production in the upper 25 m to photic zone integrated production was higher in the AS than the SIO due to low nutrients in the upper water column in the latter basin. Depth of nitracline showed inverse relation with primary production and *f*-ratios (ratio of new to primary production) in the study region. Insignificant differences in mean primary production and *f*-ratios were observed in the AS during 2015 (present study) as compared to a 1995 study, contradicting the belief that rapid warming may modify primary production.

Key words: Primary production, new production, nutrients, phytoplankton biomass, Indian Ocean

1. Introduction

Annual phytoplankton production in the ocean accounts for about half of the Earth's primary production and it is the main source of energy to heterotrophs. Primary production not only supports carbon demand in the surface waters, but also that in the deep ocean layers through export. The new production in the surface mixed layer determines the amount of export production to deeper layers (Eppley and Peterson, 1979). The magnitude of primary and export productions determines the amount of carbon dioxide removed from the atmosphere (Turner, 2015). The export production to subsurface waters is one of the major governing processes that determines the intensity of the oxygen minimum zone (OMZ; McCreary et al., 2013). It is estimated that about 10% of the global net primary production is exported to the subsurface waters (Buitenhuis et al., 2013; Siegel et al., 2014). However, this fraction depends mainly on the nutrient availability, physical processes, phytoplankton composition and the hydrological conditions.

The north western Indian Ocean (Arabian Sea, AS) is one of the most highly productive regions in the world with large spatial and seasonal variability due to changing physical processes (Bhattathiri et al., 1996; Barber et al., 2001). The high production in the AS is caused by occurrence of convective mixing during winter and upwelling during the summer that bring nutrients to the photic zone. The primary production in the AS varies from 852 to 1344 mgC m⁻² d⁻¹ (Barber et al., 2001), 552 to 1032 mgC m⁻² d⁻¹ (Dickson et al., 2001), 545 to 1530 mgC m⁻² d⁻¹ (Savidge et al., 1999) and 163 to 606 mgC m⁻² d⁻¹ (Bhattathiri et al., 1996) during non-monsoon period. The variations in primary production recorded by different investigations seem to have been caused by spatial variation as Bhattathiri et al. (1996) studied in the eastern AS whereas the other studies are mainly in the western and central AS. In contrast, primary production during summer monsoon is significantly greater than non-monsoon periods due to higher nutrient inputs from subsurface waters through vertical mixing (Barber et al., 2001; Dickson et al., 2001). On the other hand, the equatorial Indian Ocean and South Indian Ocean (SIO) are low productivity regions due to the absence of equatorial upwelling (Schott and McCreary, 2001). Qasim (1977) analysed primary production data collected during International Indian Ocean Expedition (IIOE) and reported that higher surface primary production in the Bay of Bengal (BoB) was due to supply of nutrients through river discharge than in the AS and the SIO. In contrast, the annual mean depth integrated primary production to the photic zone was 1.5 times higher in the AS than in the BoB and the SIO and such higher production in the AS has been found in the Oman and Somalia coastal regions due to strong upwelling (Barber et al., 2001). Barber et al. (2001) found that primary production in the AS is the highest in the Indian Ocean. Gauns et al. (2005) compared primary production in the AS and BoB with limited data and

found that AS was highly productive compared to BoB due to strong stratification and less nutrients inputs to the latter.

McCarthy et al. (1999) estimated new production in the AS using isotopically enriched nitrogen tracers during winter (January-February 1995) and post (fall) monsoon (October-November 1995) periods. They found that new production varied from 52 to 665 and 31 to 406 mgC m⁻² d⁻¹ in the AS during winter and post monsoon periods, respectively. The estimated *f*-ratio (ratio of new to total production) varied from 0.01 to 0.31 and 0.04 to 0.29, respectively, during winter and post monsoon periods. Gandhi et al. (2010) measured new production of ~53 to 152 mgC m⁻² d⁻¹ with *f*-ratios of 0.69 - 0.83 during premonsoon (April) period in the eastern shelf of AS and high *f*-ratios are attributed to occurrence of nitrogen fixation. However, these measurements are mainly restricted to the shelf region of east coast of AS (Gandhi et al., 2010).

Upper ocean particulate organic carbon flux exported to the subsurface layers (>100 m) has been estimated using particle reactive Thorium-234 in the AS and found to be 5-10% of the primary production (Buesseler et al., 1998). The highest ratio of particle flux to primary production (17-28%) is observed during post monsoon period in the AS (Buesseler et al., 1998). Recently Anand et al. (2018) found that <10% of the primary production is exported to depths below 100 m in the AS during premonsoon (March to April). The fraction of the primary production exported to subsurface layers in the AS is found to be higher (5-10%) than in BoB (2-5%), which is attributed to microplankton contributing to primary production in the AS (Ownes et al., 1993; Anand et al., 2017; 2018) against picophytoplankton contributing in the BoB (Sherin et al., 2018). To our knowledge, since IIOE (Qasim, 1977), there have been no further reports on productions of primary, new, regenerated and export are available from the SIO.

Recently Roxy et al. (2014) concluded that Indian Ocean is warming up rapidly and that summer monsoon is becoming weaker in recent years due to climate change, which may have begun to result in a decrease in primary production in the Indian Ocean. On the other hand, satellite Chl-*a* in the AS and equatorial Indian Ocean is observed as increasing from the 1970's to early 2000's (Gregg et al., 2003). Consistent with Roxy et al.'s observation, Gregg et al. (2017) observed a decline in Chl-*a* trend in the North and equatorial Indian Ocean, based on 18 years satellite Chl-*a* (1998-2015) data and based on numerical models, and they attributed it to a decline in diatoms and chlorophytes and increase in cyanobacteria. Due to lack of long-term *in situ* data, the dichotomy could not be resolved. The objective of this study is to 1) examine the spatial variability in the primary, new and regenerated production in the north western Indian Ocean, 2) estimate *f*-ratios and evaluate potential reasons for their variability during post-monsoon period and 3) examine the possible changes in

primary production and f -ratios in the Indian Ocean in the past two decades by comparing data collected during 1995 under Joint Global Flux Study (JGOFS) and present study (2015).

2. Material and methods

2.1. Sampling

Seawater samples were collected in the Indian Ocean as a part of Indian GEOTRACES program, two cruises were conducted on board ORV Sagar Kanya (Cruise No. SK- 324 and 325) between India and with Goa-Mauritius and Chennai transects (Figure 1). Cruise (SK 324) started on 22 September 2015 at Goa, India and reached Port Luis on 20 October 2015 and then reached Chennai on 20 November 2015 covering a wide range of oceanographic settings from the low productivity SIO (5°S-25°S) to the highly productive AS (along ~59°E) in the Indian Ocean.

Vertical profiles of salinity, temperature, dissolved oxygen, fluorescence and photosynthetic active radiation (PAR) were measured *in situ* using sensors attached to clean ultra-trace metal free CTD-Rosette system (SeaBird Electronics, USA). Density of water column was estimated using *in situ* temperature, salinity and pressure. After subtracting 0.5 °C from the temperature profiles, the density was estimated again. The depth of MLD was taken where the difference in density of *in situ* temperature and density after subtracting 0.5°C was zero (Shenoi et al., 2004; Shankar et al., 2016). The depth of photic zone was estimated as the depth that coincided with 0.1% of surface PAR. Water samples from the Niskin bottles were sub-sampled into 60 ml glass stoppered bottles and care was taken to avoid trapping of air bubbles for dissolved oxygen (DO). The DO was measured using Winkler titration method following potentiometric detection (Carritt and Carpenter, 1966) using potentiometer (Titrande Metrohm, Zofingen, Switzerland). Nutrient concentrations were measured by colorimetric techniques following Grasshoff et al. (1992). The precisions of nitrate, ammonium, phosphate and silicate were ± 0.02 , 0.02, 0.01 and 0.02 μM , respectively. About 5-10 L of water was passed through a 0.7 μm GF/F filter and the Chl-*a* retained on the filter was extracted into 90% acetone, and measured using High Performance Liquid Chromatography (HPLC; 1200 series, Agilent Technologies, USA) following Roy et al. (2015).

2.2. In Vitro Primary Production Measurements

Seawater samples were collected at six light depths where 100%, 90%, 75%, 50%, 25% and 1% of surface PAR occurred at 21 stations along the cruise track with 7 stations in the SIO and 14 stations in the AS for primary productivity and new production. The primary production in seawater at different depths was measured by spiking enriched sodium bicarbonate ($\text{NaH}^{13}\text{CO}_3$; 99%; Sigma Aldrich, USA) and its uptake by phytoplankton was measured following the procedures given by

Hama et al. (1983). Briefly, seawater samples were collected from different light depths in Nalgene transparent bottles and 0.2 mL of 2 mM of ^{13}C enriched sodium bicarbonate spike added to one litre of sample in triplicates of light and dark bottles and incubated in the deck incubator. The temperature in the incubator was maintained with running surface seawater. Different light screens were used to maintain light intensities representative for the deeper samples. Samples were incubated for 24 h and were filtered through pre-combusted GF/F filters in the same manner as for POC samples. The POC filters were frozen at -20°C after filtration on board the research vessel. In the shore laboratory, the filters were dried overnight at 50°C and the filter was acid-fumed (HCl) for 12 h to remove inorganic carbon, and then dried again for analyses of the organic carbon content and isotopic composition. The change in the isotopic composition of the carbon was measured using elemental analyzer coupled to an isotope ratio mass spectrometer (IRMS; Delta V Plus, Thermo Electron, Germany).

The initial isotopic composition of carbon was measured by filtering the sample soon after addition of spike. The computation of primary production from the concentration of POC and isotopic enrichment were done following Hama et al. (1983). The precision of primary production in terms of the CV was 5%.

2.3. *In Vitro new and regenerated production measurements*

One litre of seawater sample was taken from 6 light depths (same as in primary production measurements) in transparent polycarbonate Nalgene bottles. Incubation was initiated after adding trace quantities of ^{15}N labelled (99 at%) NaNO_3 and NH_4Cl in different bottles. Nutrients data of each sample were used to determine the quantity of ^{15}N addition. The target level was 10% of ambient nutrient concentration. All experiments were conducted in triplicate. The samples were immediately placed in deck-board incubators with flowing surface seawater to prevent solar heating and light screens to simulate *in situ* light levels. Incubations were terminated by filtration on combusted Whatman GF/F filters (McCarthy et al., 1996).

Isotopic composition of nitrogen was measured using an Isotope Ratio Mass Spectrometer in the same way as mentioned for ^{13}C for primary productivity. Isotope tracer techniques with ^{15}N labelled substrates were used to obtain rates of nitrate and ammonium uptake following standard protocols (McCarthy et al., 1984; 1996; 1999). Ammonium uptake rates were corrected for isotope dilution as per Garside and Glibert (1984) and all uptake rates are expressed as ρ . The f -ratios were computed as the ratio of new production to total primary (new + regenerated) production following McCarthy et al. (1996). In order to minimize uncertainties arising from growth, grazing and potential depletion of nutrients, incubations were conducted for 4 h duration. At each station, 4 samples with enriched

nitrate and 4 samples with enriched ammonium were incubated through four hour duration in five batches during 0600-1000h, 1000-1400h, 1400-1800h, 1800-2200 and 2200-0200 h. Daily rates of nitrogen uptake were computed by summing the uptake rates for both day and night time. The precision of the atomic ratio (at%) was 0.007 and particulate nitrogen is 0.05 μM .

2.4. Satellite Data

Sea surface temperature (SST), salinity (SSS), Chlorophyll-a (Chl-a), sea surface height anomaly (SSHA) and geostrophic currents in the study region were mapped from satellite observations to examine the water conditions and identify specific features such as eddies. The monthly mean SST (spatial resolution of 4 km^2), SSS (0.5 x 0.5 $^\circ$), SSHA (0.25 x 0.25 $^\circ$), and geostrophic currents (0.25 x 0.25 $^\circ$) were obtained from Copernicus Marine Environmental Monitoring Service (www.marine.copernicus.eu) (Figure 1). The SSHA and geostrophic currents on the day of sampling of each station are given in Supplementary Figure S1.

3. Results

3.1. Spatial variations in hydrographic parameters in the western Indian Ocean

Mean sea surface temperature, salinity, Chl-a, merged sea surface height anomaly (SSHA) and geostrophic currents in the Indian Ocean are shown in Figure 1a–d for the study period (September–October 2015). Equatorial region is warmer compared to north and south of Indian Ocean where relatively cooler waters were observed in the south of 10 $^\circ\text{S}$ (Fig. 1a). Salinity was higher by up to 0.5 psu in the eastern (stn. 3-6) than the western AS (stn. 8-17) that decreased towards SIO (Fig. 1b). Higher Chl-a was observed in the western AS in association with low temperature compared to other study region. Chl-a in the SIO was a little over 50% of that of AS (Fig. 1c). Variations in merged SSHA and geostrophic surface currents in the Indian Ocean showed an increase in SSHA by 0.2 m in the western AS and south of equator (Fig. 1d). Though several cyclonic and anticyclonic eddies were found in the study regions, the sampling was done only outside the eddy regions (Supplementary Figure S1) to represent and compare normal oceanographic features.

The water column was thermally stratified in the study region with temperature gradients of 4 to 7 $^\circ\text{C}$ between upper 40-80 m and depths below (Fig. 2a). The depth of 26 $^\circ\text{C}$ isotherm was at about 55 m in the north that deepened to ~80 m to the south of 9 $^\circ\text{S}$. Similarly, higher salinity (by ~0.75 psu) was observed to the north of 12 $^\circ\text{N}$, which decreased southward with weak vertical salinity gradients (Fig. 2b). Relatively low salinity was observed in the coastal than offshore regions. Chl-a in the upper 20 m of water column was mostly <0.15 mg m^{-3} but with higher surface values (>0.15 mg m^{-3}) to the north of 15 $^\circ\text{N}$ in the coastal AS (stn 5, 6) and 9 $^\circ\text{S}$ (Stn 17) (Fig. 2c). Prominent subsurface Chl-a

maximum (0.2 to 0.5 mgm⁻³) was observed in the entire study region, but was weaker to the south of 9° S (0.1-0.15 mg m⁻³; stn. 18-21). The highest subsurface Chl-*a* maxima with >1.5 mg m⁻³ were observed between 10 and 20°N (stns. 8-11). The subsurface Chl-*a* maxima were shallower in the north that deepened in the south. The photic zone integrated Chl-*a* ranged between 6.2 and 64.6 mg m⁻² in the study region with higher concentrations in AS (42.5±3 mg m⁻²) than in SIO (31.6±4 mg m⁻²) (Table 1). Photic zone integrated primary production showed significant positive relation with that of photic zone integrated Chl-*a*, except in coastal waters (stns. 1-3) (Fig. 5; r²=0.68; p<0.001). Dissolved oxygen (DO) in the upper 50 m of water column ranged between 170 and 228 µM with relatively low concentrations in AS than in SIO (Fig. 2d). DO concentration below 85 m were significantly lower (<100 µM) in the AS but was higher in the SIO (>100 µM). The lowest DO concentrations were observed at depth greater than 50 m in coastal waters (stn 1-3) and the northern Arabian Sea (17-21°N; Stns. 7-8) and were associated with cooler waters. The vertical boundary of low DO zone mostly followed the depth of thermocline (Fig 2d). The photic zone varied between 89 and 123 m in the open sea regions with deepening from north to south.

The concentration of dissolved nitrate was 0.5 to 1.0 µM in the upper 25 m of water column in coastal region in the AS (Stn. 1-3). The depth of <0.5 µM of nitrate was shallow in the AS (20 m) and deepened towards SIO to 80 m (Fig. 3a). The depth of nitracline (represented by 2 µM isoline) occurred at 15 m in the north and deepened to 82 m in the south (9° S) but it was below 100 m in the region north of 9° S. The mean concentration of nitrate in the photic zone was higher in AS (5.6±3µM) than in SIO (0.8±0.2µM). In contrast, the concentration of ammonium in SIO in the photic zone was higher than in AS (Fig. 3b). Both phosphate and silicate concentrations were higher in the AS compared to that in SIO (<0.5 µM) (Fig. 3c, d). The depth of 2 µM silicate isoline was below 30 m in the AS, except in coastal region, and south of equator. Enhanced phosphate and silicate were observed in the upper 40 m of water column in equatorial region. The mean concentration of silicate in the photic zone was higher in AS (4.2±2 µM) than SIO (3.0±2 µM).

3.2. Spatial variation in new and regenerated production in the western Indian Ocean

The nitrate and ammonium uptake rates varied between 0.02 and 3.2, and 0.08 and 11.65 mgN m⁻³ d⁻¹, respectively, in the photic zone. The depth (photic zone) integrated nitrate and ammonium uptake rates varied from 13.3 to 58.8 and 85.6 to 406.7 mgN m⁻² d⁻¹ respectively (Table 1). The nitrate and ammonium uptake rates were converted to new and regenerated production using Redfield's C/N ratio of 6.6. The new production in the western Indian Ocean varied between 0.13 and 71.3 mgC m⁻³ d⁻¹ during the study period and relatively higher production was observed in equatorial region

(between 10° N and 10° S). The photic zone integrated new production ranged from 87.8 to 398.0 mgC m⁻² d⁻¹ (Table 1) and it was nearly the same in AS (245.5±297 mgC m⁻² d⁻¹) and in SIO (264±165 mgC m⁻² d⁻¹) (Fig. 4a; Table 2). In contrast, regenerated production was lower in the AS (1254±574 mgC m⁻² d⁻¹) than in SIO (1933±838 mgC m⁻² d⁻¹) (Fig. 4b). The depth of nitracline showed significant linear relation with photic zone integrated new ($r^2=0.47$; $p<0.001$) and regenerated production ($r^2=0.48$; $p<0.001$) in the study region (Fig. 6a,b). But the depth integrated (photic zone) regenerated production was higher by a factor of 3.6 to 14.1 compared the new production (Table 2).

3.3. Spatial variation in primary production in the western Indian Ocean

The primary productivity in the surface waters varied between 5 and 48 mgC m⁻³ d⁻¹ in the study region. The lowest surface production was noticed in coastal waters of the AS (stns 1 and 2) and in the SIO (stn 18 and 21). The depth integrated primary production in the photic zone varied between 229 and 1900 mgC m⁻² d⁻¹ in the Indian Ocean with relatively higher production in the AS than in the SIO (Fig. 4c). The mean photic zone integrated primary production was higher in the AS (1238±626 mgC m⁻²d⁻¹) than in SIO (675±431 mgC m⁻²d⁻¹) (Table 1). The photic zone integrated Chl-*a* showed significant linear relation with photic zone integrated primary production (Fig. 5). The depth of nitracline displayed significant negative relation with primary production (regression model II; $r^2=0.42$; $p<0.001$; Fig 6c) and positive relation with temperature (regression model II; $r^2=0.77$; $p<0.001$; Fig. 6e) in the study region (Fig. 6a-c), except in coastal regions (stn 1-3). The photic zone integrated primary production showed inverse relation with photic zone mean N/P ratio (Fig. 6f). The *f*-ratio varied between 0.08 and 0.26 with relatively higher values *f*-ratios in the AS (0.144±0.06) than in SIO (0.122±0.05; Table 1). The *f*-ratios showed linear relation with photic zone mean temperature and integrated Chl-*a* (Fig. 6g,h) and inverse relation with depth of nitracline (Fig. 6d).

4. Discussion

4.1. Variability in nutrients concentrations in the western Indian Ocean

The water column temperature suggests that waters were thermally stratified in the western Indian Ocean, especially to the north of 9° S (Fig. 2a). Higher salinity was observed in the north western Indian Ocean due to high evaporation over precipitation (Prasad et al., 1997) leading to formation of Arabian Sea High Saline waters during the winter (Fig. 2b). The mixed layer was deeper in the SIO (57±15 m) than in AS (35.7±8 m). The depth of mixed layer generally governs nutrient concentrations in the upper ocean. As a result, relatively lower nutrients concentrations were observed in the upper 80 m of water column in the SIO than in the AS (Fig. 3a-d). The

concentrations of silicate were higher in the coastal AS and equatorial Indian Ocean than in the SIO and open ocean region of the AS. Such high concentrations of silicate were also found in the equatorial region that may possibly be due to advection of BoB waters from east to western equatorial Indian Ocean (Schott and McCreary, 2001). Nevertheless, existence of stronger heterotrophy is expected in the SIO than in the AS due to lack of nutrients in the upper 80 m of water column (Fig. 3). Relatively lower nitrate and higher phosphate concentrations with low N/P ratio (2.7 ± 2) were observed in the mixed layer indicating possible nitrogen fixation (Fig. 3a, d). The isotopic composition of particulate nitrogen ($\delta^{15}\text{N}_{\text{PN}}$) in the study region was higher (4.8 to 7 ‰; Sherin, 2019) than expected if nitrogen fixation occurred (0 ‰) suggesting that nitrogen fixation can be negated as a dominant mechanism of organic matter formation. Sherin et al. (2018) found lighter nitrogen isotopic composition in the particulate nitrogen (3-4 ‰) in the BoB during fall (post) monsoon (November-December) and suggested that phytoplankton may utilize dissolved organic nitrogen (DON) as an alternative source of nitrogen. In contrast, the higher $\delta^{15}\text{N}_{\text{PN}}$ (4.8-7 ‰) indicates low contribution of DON as a nitrogen source to phytoplankton productivity during the study period. However, further study is needed to examine the role of nitrogen fixation and utilization of DON in this region.

Though nutrients in the upper ocean were low in the western Indian Ocean, the photic zone integrated nutrients increased progressively from south to north, for example for nitrate, from 17.9 to 1392 mmol m^{-2} . The photic zone integrated nitrate was higher in AS ($703\pm 220 \text{ mmol m}^{-2}$) than in SIO ($108\pm 68 \text{ mmol m}^{-2}$) (Table 1). Similarly photic zone integrated phosphate was also higher in AS ($70.5\pm 13 \text{ mmol m}^{-2}$) than SIO ($47.0\pm 14 \text{ mmol m}^{-2}$).

4.2. Influence of water column nutrients on new and regenerated production

The photic zone integrated new and regenerated production varied from 87.8 to 600 and 565 to 2684 $\text{mgC m}^{-2} \text{d}^{-1}$, respectively, in the Indian Ocean. The mean new and regenerated production in the AS (179 ± 86 and $1204\pm 582 \text{ mgC m}^{-2} \text{d}^{-1}$ respectively) and in the SIO (203 ± 90 and $1654\pm 263 \text{ mgC m}^{-2} \text{d}^{-1}$ respectively; Table 1) suggests that new production may be similar but the regenerated production is significantly higher in the SIO than in the AS ($t_{\text{stat}}=-3.1$; $p<0.01$). The primary production in the Indian Ocean is in the same range measured in the tropical Pacific (210-1179 $\text{mgC m}^{-2} \text{d}^{-1}$, except in Peruvian upwelling region (Pace et al., 1987; Bouteiller et al., 2003; Pennington et al., 2006) and Atlantic Ocean (130-1320 $\text{mgC m}^{-2} \text{d}^{-1}$ during winter and autumn (Vinogradov et al., 1997; Maranon et al., 2003; Tilstone et al., 2009). The mean new production in the AS during the present study ($179\pm 86 \text{ mgC m}^{-2} \text{d}^{-1}$) agrees with that during 1995 ($138.6\pm 39 \text{ mgC m}^{-2} \text{d}^{-1}$; McCarthy et al., 1999).

The depth of nitracline showed significant positive relations with both new ($r^2=0.47$; $p<0.001$; Fig. 6a) and regenerated production ($r^2=0.48$; $p<0.001$; Fig. 6b) in the western Indian Ocean. When depth of the nitracline is deeper, the concentration of nutrients in the upper water column is significantly lower and addition of nutrients from external sources (tracer nutrient) would increase new production and this would be one of the draw backs of the tracer method. The photic zone integrated nitrate, and phosphate showed positive relation with primary production (Fig. 7a, d) whereas negative relation with new production and regenerated production in the western Indian Ocean (Fig. 7b-c, e-f). The photic zone integrated silicate did not show significant relation with new and regenerated production, despite silicate concentration in the mixed layer being lower than the limiting concentrations ($<2 \mu\text{M}$) (data not shown), which suggests that non-silicious phytoplankton may be contributing to the production.

4.3. Influence of water column characteristics on Primary production

The photic zone integrated Chl-*a* is higher in the AS ($42.5\pm 3 \text{ mg m}^{-2}$) than in the SIO ($31.6\pm 4 \text{ mg m}^{-2}$). As a result, the photic zone integrated primary production was also higher in the AS ($1238\pm 626 \text{ mg C m}^{-2} \text{ d}^{-1}$) than in the SIO ($675\pm 431 \text{ mg C m}^{-2} \text{ d}^{-1}$; Table 1). The photic zone integrated primary production of water column showed significant linear relation with photic zone integrated Chl-*a* in the entire study region suggesting that the phytoplankton biomass nearly represents primary production in the study region (Fig. 5). The contribution of upper 25 m water column primary production to column production (100 m) was higher ($45\pm 5\%$) in AS but it was lower in SIO ($28\pm 6\%$) which appears to have been mainly caused by availability of high concentrations of nutrients in the AS.

Both mixed layer mean nutrients and Chl-*a* did not show significant relation with photic zone integrated primary production. In contrast, photic zone integrated nutrients displayed significant linear relation with photic zone integrated primary production (Fig. 7) suggesting that occurrence of nutrients below the mixed layer is important for primary production. Similarly the depth of nitracline showed inverse relation with primary production as deeper nitracline leading to less nutrients available for primary production (Fig. 6c). The photic zone integrated Chl-*a* showed linear relation with photic zone integrated primary production suggesting that subsurface Chl-*a* contributed significantly to the primary production (Fig. 5). The subsurface Chl-*a* maximum occurrence mostly above 40 m, where significant amount of light penetrates contributed significantly to primary production.

4.4. Comparison of PP by models and measurements

The primary production is estimated using remote sensing measured surface properties of ocean (Behrenfeld and Falkowski, 1997; Behrenfeld et al., 2005; Westberry et al., 2008). The Vertically Generalized Production Model (VGPM) uses remote sensing of sea surface temperature, surface chlorophyll-a, photosynthetic active radiation and day length data to estimate primary production in the euphotic zone. In this model phytoplankton biomass normalized primary production (pB) is derived from its relationship with sea surface temperature following Behrenfeld and Falkowski (1997). The Carbon based Productivity Model (CbPM) is an improved model over the VGPM mainly for the depth of euphotic zone and using particulate backscatter and phytoplankton absorption coefficients instead of Chlorophyll-a based (Behrenfeld et al., 2005 and Westberry et al., 2008). The mean primary productivity estimated based on VGPM and CbPM models were significantly lower in the study region than *in situ* primary production by 35 and 58%, respectively, in the AS and the equatorial Indian Ocean whereas their results were over estimated by 50% and 10% respectively in the SIO (Fig. 8a,b). Especially higher deviations between measured and models (both CbPM and VGPM by 40-52% and 60-85% respectively) occurred in the region between 1°S to 12°N and it is less in other regions (Fig. 8b). Notably VGPM and CbPM estimated equally the measured PP in the SIO (by 42±20%) whereas CbPM estimated better in the Arabian Sea (63±18%) than VGPM (43±13%) (Fig. 8b). This suggests that the both models are performing equally in low Chl-a regions but CbPM is reproducing well in the high Chl-a regions (Fig. 8b). Such differences between measured and modelled results may be due to time-scales of integration as *in situ* measurements are daily mean whereas model data are monthly means. The monthly variability in the Chl-a in open ocean regions is expected to be small during inter-monsoon period due to stratification. Even if the variability is considered to be within 10%, the models are able to reproduce up to 40-60% of *in situ* production in the Indian Ocean. These models are used in the potential fishery zone predictions in the Indian Ocean and a caution needs to be exercised when using these predictions as models are weakly reproducing true primary production. The primary production models could be refined with the inclusion of seasonal nutrient inputs, stratification, and grazing in to consideration. Inclusion of more *in situ* primary production data from this region may improve the model performance further through improved calibration of models.

4.5. Comparison of new production and f-ratio with measured sinking fluxes

The new production is expected to be equivalent to exportable production from the photic to the twilight zone as they are averaged over a period in which steady state is assumed (Eppley, 1989). Based on the sinking fluxes estimated using particle reactive ²³⁴Th and primary production,

Buesseler et al. (1998) observed that 4.8 to 22.1% of the primary production is exported to the subsurface layers during late SW monsoon in the open ocean region of the AS. Recently Anand et al. (2018) observed 1.4 to 4% of primary production is exported to the subsurface layers (>100 m) during premonsoon (March-April, 2014) in the AS. The present study suggests that the new (^{15}N) production accounts to 1 to 11.2% (mean: 3.5%) of the primary production (^{13}C) in the AS and 1.4 to 8.8% (mean: 6%) in the SIO. The mean new production to total production ratio ($3.5\pm 1\%$) is close to the export production at 100 m depth using particle associated ^{234}Th tracer (Anand et al., 2018). On the other hand, f -ratios in the study region ranged from 0.08 to 0.26 with means of 0.144 ± 0.06 and 0.122 ± 0.04 in the AS and SIO, respectively, during the study period (based on their $^{15}\text{N}_{\text{NO}_3}$ production divided by sum of $^{15}\text{N}_{\text{NO}_3}$ and $^{15}\text{N}_{\text{NH}_4}$ production). The mean f -ratio is supposed to reflect the fraction of primary production exported to the subsurface layers over a period of several months (Eppley and Peterson, 1979). However, the mean f -ratio (Table 1) suggests that ~14% of the primary production is exported to layers below 100 m in the AS and 12% in the SIO, which is only slightly higher than the mean ratio of new production to total production (new and regenerated production by ^{15}N method). This small difference could possibly be due to underestimation of total production by ^{15}N tracer method due to non-inclusion of organic nitrogen production. Gandhi et al. (2010) reported uptake of organic nitrogen using ^{15}N -urea and that increased f -ratios by ~10% in the coastal AS during spring intermonsoon (March-April). Hence the derived f -ratios based on the new production by $^{15}\text{N}_{\text{NO}_3}$ and total production by ^{13}C tracer seem to be underestimates. Nevertheless, this study suggests that the fraction of new production to total production (3.5%) is close to that of export production estimated using ^{234}Th tracer (~3%; Anand et al., 2018). The mean production during USJGOFS (1995) has been $1371\pm 132 \text{ mg C m}^{-2} \text{ d}^{-1}$ (Barber et al., 2001) which is not very different from that observed in the present study ($1238\pm 626 \text{ mgC m}^{-2} \text{ d}^{-1}$), which indicates that the basin-wide mean new and primary production did not significantly change in the past two decades during post monsoon season (September-October). The mean f -ratio during the study period (based on ^{15}N tracer of NO_3 and NH_4) in the AS amount to 0.144 ± 0.06 in the present study, which is consistent with the mean f -ratio measured in October-November 1995 (0.145 ± 0.07) in the AS during the US JGOFS program using the same method. The range of f -ratios estimated in the Indian Ocean are within the range measured in the Pacific (Dugdale and Wilkerson, 1998; Dugdale et al., 2011; Parker et al., 2011; Rafter et al., 2017) and Atlantic Ocean (Dauchez et al., 1996; Metzler et al., 1997). Prakash et al. (2012) analysed remote sensing Chl-*a* in the AS from 1997-2010 and found no secular trends on the basin-scale during spring/fall inter monsoon period. Variability, however, has been observed during other periods in the AS and attributed to decadal oscillations in physical processes including

sea level anomaly, wind driven mixing etc. In contrast, Gregg et al. (2017) found a decline in Chl-*a* trend in the north and equatorial Indian Ocean between 1998 and 2016. Roxy et al. (2014) argued that rapid warming of Indian Ocean due to climate change resulted in a weaker summer monsoon that may decrease primary production in the Indian Ocean and hence lower *f*-ratios. Breitbart et al. (2018) found absence of long-term trends in oxygen minimum zone (OMZ) in the Indian Ocean further indicating that weak or insignificant changes in primary production had taken place, as otherwise the intensity of the OMZ would be altered via export of organic matter. The present study compares only two data sets collected two decades apart and that data may be biased due to sampling period and seasonal variability as also spatial variability. Therefore, long-term data sets are required to generate in order to confirm the inferences made here and also to examine climate change influence on biological production in the Indian Ocean.

5. Summary and Conclusions

To examine the spatial variability in new, regenerated and primary productions; samples were collected at 21 stations in the western Indian Ocean under Indian-GEOTRACES program. High concentrations of nutrients were found in the upper 30 m of water column in the Arabian Sea (AS) due to advection of nutrient-rich coastal upwelled waters from Oman and Somalia coasts. Chl-*a* in the upper 25 m was low with occurrence of prominent subsurface Chl-*a* maximum between 25 and 50m in the western Indian Ocean. The mean new production was same in the AS and South Indian Ocean (SIO), north of 30°S, but the regenerated production was higher in the latter. The photic zone integrated nutrients displayed weak relationship with new production whereas strong relation was observed with regenerated nutrients (nitrate and phosphate) in the study region. The photic zone integrated primary production was more than double in the AS ($1238 \pm 626 \text{ mg C m}^{-2} \text{ d}^{-1}$) compared to the SIO ($674 \pm 431 \text{ mg C m}^{-2} \text{ d}^{-1}$) with significant linear relation with photic zone integrated Chl-*a* in the entire study region. The upper 25m of water column contributed ~45% and 28% of primary production to the photic zone in the AS and in SIO, respectively, suggesting that production in the deeper portion of the photic where nutrient concentrations are greater than in the surface portion of the photic zone. The photic zone integrated nutrients and Chl-*a* displayed significant linear relationship with photic zone integrated primary production suggesting that nutrients below the mixed layer support significant column production. The mean production during Fall-monsoon period in the present study during 2015 ($1238 \pm 626 \text{ mgC m}^{-2} \text{ d}^{-1}$) is not statistically significantly different from that during 1995 under USJGOFS program ($1371 \pm 132 \text{ mgC m}^{-2} \text{ d}^{-1}$). Similarly, the mean *f*-ratios during the present study in the AS (0.144 ± 0.06) is also not different during similar period in 1995 (0.145 ± 0.07) suggesting that contrary to the hypothesis of rapid decrease in primary

production in recent times due to climate change, no recognisable modifications to water column primary production was observed in the AS over the past two decades.

Acknowledgements: We would like to thank Prof. S.K. Singh for his co-ordination of the Indian-GEOTRACES team. We would like to thank Chief Scientist and Physical Research Laboratory team for their help during sampling and operation of CTD. We would like to thank Ministry of Earth Science for funding and ship time of ORV Sagar Kanya. HD acknowledges Senior Research Fellow (SRF) from Council of Scientific and Industrial Research (CSIR). We would like to thank three anonymous reviewers and Associate Editor Prof. Craig Carlson for their critical review to improve the presentation of manuscript. The data used in this manuscript are available at National Oceanographic Data Centre (NODC) of CSIR-National Institute of Oceanography (www.nio.org/NODC).

References

- Anand, S.S., Rengarajan, R., Sarma, V.V.S.S., Sudheer, A.K., Bhushan, R., and Singh, S.K.(2017). Spatial variability of upper ocean POC export in the Bay of Bengal and the Indian Ocean determined using particle-reactive ^{234}Th . *J. Geophys. Res. Oceans*, 122, doi: 10.1002/2016JC012639.
- Anand, S.S., Rengarajan, R., Sarma, V.V.S.S. (2018). ^{234}Th based carbon export flux along the Indian GEOTRACES GI02 section in the Arabian Sea and the Indian Ocean. *Global Biogeochem. Cycles*, doi: 10.1002/2017GB005847
- Barber, R. T., J. Marra, R. C., Bidigare, L. A. Codispoti, D. Halpern, Z. Johnson, M. Latasa, R. Goericke, and S. L. Smith. (2001). Primary productivity and its regulation in the Arabian Sea during 1995, *Deep Sea Res., Part II*, 48, 1127–1172.
- Behrenfeld, M.J. and Falkowski, P.G. 1997. Photosynthetic rates derived from satellite-based chlorophyll concentration. *Limnol. Oceanogr.*, 42, 1-20.
- Behrenfeld, M.J., Boss, E., Siegel, D.A., Shea, D.M. 2005. Carbon-based ocean productivity and phytoplankton physiology from space. *Global Biogeochem. Cycles*, 19, 1006, doi: 10.1029/2004GB003399.
- Bhattathiri, P. M. A., Pant A., Sawant, S., Gauns, M., Matondkar, S. G. P., and Mohanraju, R. 1996 Phytoplankton production and chlorophyll distribution in the eastern and central Arabian Sea in 1994--1995; *Curr .Sci.* **71** 857--862
- Bouteiller, A.L., Leynaert, A., Landry, M.R., Borgne, R.L., Neveux, J., Rodier, M., Blanchot, J., and Brown, S.L. 2003. Primary production, new production, and growth rate in the equatorial Pacific: Changes from mesotrophic to oligotrophic regime. *J. Geophys. Res.*, 108, 8141, doi:10.1029/2001JC000914.
- Breitburg, D., Levin, L.A., Oschlies, A., Gregoire, M., et al., 2018. Declining oxygen in the global Ocean, *Science*, 359, 1-11.

- Buitenhuis, E. T., T. Hashioka, and C. L. Quere (2013). Combined constraints on global ocean primary production using observations and models, *Global Biogeochem. Cycles*, 27, 847–858, doi:10.1002/gbc.20074.
- Buesseler, K.O., Ball, L., Andrews, J., Benitez-Nelson, C., Belostock, R., Chai, F., and Chao, Y. (1998). Upper ocean export of particulate organic carbon in the Arabian Sea derived from Thorium-234. *Deep-Sea Res.*, II, 45, 2461-2487.
- Carritt, D. E., and J. H. Carpenter (1966). Comparison and evaluation of currently employed modifications of the Winkler method for determining dissolved oxygen in seawater; a NASCO report, *J. Mar. Res.*, 24, 286–318.
- Dauchez, S., Legendre, L., Fortier, L., and Levasseur, M. 1996. New production and production of large phytoplankton (>5 µm) on the Scotian Shelf (NW Atlantic), *Mar. Ecol. Prog. Ser.*, 135, 215-222.
- Dickson, M.L., Orchard, G., Barber, R. L., Marra, J., McCrathy, J.J. and Sarnbroto, R.N., (2001). Production and respiratory rates in the Arabian Sea during the 1995 northeast and southwest monsoon. *Deep Sea Res. II*, 48: 1199-1230.
- Dugdale, R. C. & Wilkerson, F. P. 1998. Silicate regulation of new production in the equatorial Pacific upwelling. *Nature* 391, 270–273.
- Dugdale, R. et al. 2011. The regulation of equatorial Pacific new production and pCO₂ by silicate-limited diatoms. *Deep Sea Res. Part II Top. Stud. Oceanogr.* 58, 477–492.
- Eppley, R.A., and B.J. Peterson. 1979. Particulate organic matter flux and planktonic new production in the deep ocean. *Nature*. 282, 677-680.
- Eppley, R.A., 1989. New production: History, methods, problems, in productivity of the ocean: Present and past, edited by V.S. Smetacek, and G. Wefer, pp. 85-97, John Wiley.
- Gandhi, N., Ramesh, R., Srivastava, R., Sheshshayee, M.S., Dwivedi, R.M., Raman, M., (2010). Nitrogen uptake rates during spring in the NE Arabian Sea. *International J Oceanogra.* 127493.
- Gauns, M., Madhupratap, M., Ramaiah, N., Jyothibabu, R., Fernandes, V., Paul, J.T., Prasanna Kumar, S., (2005). Comparative accounts of biological productivity characteristics and estimates of carbon fluxes in the Arabian Sea and Bay of Bengal. *Deep-Sea Res.*, II 52, 2003-2017.
- Garside, C. and P. M. Gilbert (1984). Computer modeling of ¹⁵N uptake and remineralization experiments. *Limnology and Oceanography*, 29, 199-204.
- Grasshoff, K., M. Ehrhardt, and K. Kremling (Eds.) (1992). *Methods of Seawater Analysis*, 634 pp., Verl. Chem., Weinheim, Germany, doi:10.1002/9783527613984.
- Gregg, W.W. , Conkright, M.E., Ginoux, P., O'Reilly, J.E., Casey, N.W. 2003. Ocean primary production and climate: Global decadal changes, *Geophys. Res. Lett.*, 30, 1809, doi:10.1029/2003GL016889.
- Gregg, W.W., Rousseaux, C.S., and Franz, B.A. (2017). Global trends in ocean phytoplankton: a new assessment using revised ocean colour data. *Remote sensing Letters*, 8, 1102-1111.

- Hama, T., T. Miyazaki, Y. Ogawa, T. Iwakuma, M. Takahashi, A. Otsuki, and S. Ichimura (1983). Measurement of photosynthetic production of a marine phytoplankton population using a stable ^{13}C isotope, *Mar. Biol.*, 73, 31–36.
- Maranon, E., Behrenfeld, M.J., Gonzalez, N., Mourino, B., Zubkov, M.V. 2003. High variability of primary production in oligotrophic waters of the Atlantic Ocean: uncoupling from phytoplankton biomass and size structure. *Mar. Ecol. Prog. Ser.*, 257, 1-11.
- McCarthy, J.J. Kaplan, W., Nevins, J.L. 1984. Sources and sinks of nitrite in the water column of the York River and the Chesapeake Bay. *Limnol. Oceanogr.*, 29, 84-98.
- McCarthy J.J., Garside C., Nevins J.L. and Barber R.T. (1996). New production along 140°W in the equatorial Pacific during and following the 1992 El Nino event, *Deep-Sea Res. II*, 43,1065-1093.
- McCarthy, J.J., Garside, C., John L.N., (1999). Nitrogen dynamics during the Arabian Sea northeast monsoon. *Deep-Sea Res. II* 46, 1623-1664
- McCreary, J.P., Yu, Z., Hood, R.R., Vinaychandran, P.N., Furue, R., Ishida, A., Richards, K.J., (2013). Dynamics of the Indian-Ocean oxygen minimum zones. *Prog. Oceanogr.* 112, 15-37.
- Metzler, P.M. Glibert, T.M., Gaeta, S.A., and Ludlam, J.M. 1997. New and regenerated production in the South Atlantic off Brazil. *Deep-Sea Res.*, I, 363-384.
- Owens, N. J. P., P. H. Burkill, R. F. C. Mantoura, E. M. S. Woodward, I. E. Bellan, J. Aiken, R. J. M. Howland, and C. A. Llewellyn (1993), Size-fractionated primary production and nitrogen assimilation in the northwestern Indian Ocean, *Deep Sea Res.*, Part II, 40(3), 697–709.
- Pace, M.L., Knauer, G.A., Darl, D.M., and Martin, J.H. 1987. Primary production, new production and vertical flux in the eastern Pacific Ocean. *Nature*, 325, 803-804.
- Parker, A. E. et al. 2011. Spatial patterns of nitrogen uptake and phytoplankton in the equatorial upwelling zone (110°W - 140°W) during 2004 and 2005. *Deep Sea Res. Part II Top. Stud. Oceanogr.* 58, 417–433.
- Pennington, J.T., Mahoney, K.L., Kuwahara, V.S., Kolber, D.D., Calienes, R., Chavez, F.P. 2006. Primary production in the eastern tropical Pacific: A review. *Prog. Oceanogr.*, 69, 285-317.
- Prakash, P., Prakash, S., Rahaman, H., Ravichandran, M., and Nayak, S. 2012. Is the trend in chlorophyll-a in the Arabian Sea decreasing? *Geophys. Res. Lett.*, 39, L23605, doi:10.1029/2012GL054187.
- Prasad, T. G. (1997). Annual and seasonal mean buoyancy fluxes for the tropical Indian Ocean, *Curr. Sci.*, 73, 667–674.
- Qasim, S. Z. (1977), Biological productivity of the Indian Ocean . *Indian J. Mar. Sci.*, 6, 122–127.
- Rafter, P.A., Sigman, D.M., and Mackey, K.R.M. 2017. Recycled iron fuels new production in the eastern equatorial Pacific Ocean. *Nature*, 8, 1100, doi:10.1038/s41467-017-01219-7.
- Roy, R., Rajath, C., Vinayak, K., Krishna, M.S., Sarma, V.V.S.S., Anil, A.C., 2015. CHEMTAX-derived phytoplankton community structure associated with temperature fronts in the northeastern Arabian Sea. *J. Mar. Syst.* 144, 81–91.

- Roxy, M., K. Ritika, P. Terray, and S. Masson, (2014): The curious case of Indian Ocean warming. *J. Climate*, 27, 22, 8501-8509.
- Schott F. and McCreary J.P. (2001). The monsoon circulation of the Indian Ocean, *Progr. Oceanogr.*, 5i, 1-123.
- Sarma, V. V. S. S. and Udaya Bhaskar, T. V. S. (2018). Ventilation of Oxygen to Oxygen Minimum Zone Due to Anticyclonic Eddies in the Bay of Bengal. *Journal of Geophysical Research: Biogeosciences*, 123(7), 2145–2153. doi:10.1029/2018jg004447
- Sarma, V.V.S.S., Jagadeesan, L., Dalabehera, H.B., Rao, D.N., Kumar, G.S., Durgadevi, D.S., Yadav, K., Behera, S., Priya, M.M.R. (2018). Role of eddies on intensity of oxygen minimum zone in the Bay of Bengal. *Cont. Shelf. Res.*, 168, 48-53.
- Sarma, V.V.S.S., Yadav, K., Behera, S. 2019. Role of eddies on organic matter production and f-ratios in the Bay of Bengal, *Mar. Chem.*, 210, 13-23.
- Shankar, D., Remya, R., Vinayachandran, P.N., Charatterjee, A., Behera, A., 2016. Inhibition of mixed-layer deepening during winter in the northeastern Arabian Sea by the West India Coastal Current. *Clim. Dyn.* 47, 1049–1072.
- Shenoi, S.S.S., Shankar, D., Shetye, S.R., 2004. Remote forcing annihilates barrier layer in the southeastern Arabian Sea. *Geophys. Res. Lettrs.* 31, L05307. <http://dx.doi.org/10.1029/2003GL019270>.
- Sherin, C.K., Sarma, V.V.S.S., Rao, G.D., Viswanadham, R., Omand, M.M., and Murty, V.S.N. 2018. New to total primary production ratio (f-ratio) in the Bay of Bengal using isotopic composition of suspended particulate organic carbon and nitrogen. *Deep-Sea Res., I*, in press, doi: 10.1016/j.dsr.2018.06.002.
- Sherin, C.K. 2019. Variability in efficiency of biological pump in the Indian Ocean using stable isotopes of Carbon and Nitrogen, PhD thesis, Academy of Scientific and Innovative Research, Goa, India.
- Siegel, D. A., K. O. Buesseler, S. C. Doney, S. F. Sailley, M. J. Behrenfeld, and P. W. Boyd (2014), Global assessment of ocean carbon export by combining satellite observations and food-web models, *Global Biogeochem. Cycles*, 28, 181–196, doi:10.1002/2013GB004743.
- Tilstone, G., Smyth, T., Poulton, A., and Hutson, R. 2009. Measured and remotely sensed estimates of primary production in the Atlantic Ocean from 1998 to 2005. *Deep-Sea Res., II*, 56, 918-930.
- Turner, J. T. (2015). Zooplankton fecal pellets, marine snow, phyto detritus and the ocean's biological pump, *Prog. Oceanogr.*, 130, 205–248.
- USJGOFS 1994, Protocols for the Joint Global Ocean Flux Study (JGOFS) core measurements, UNESCO, pp: 1-181.
- Vinogradov, M.E., Shushkina, A., Vedernikov, V.I., Nezlin, N.P., and Gagarin, V.I. 1997. Primary production and plankton stocks in the Pacific Ocean and their seasonal variation according to remote sensing and field observations. *Deep-Sea Res, II*, 44, 1979-2001.

Westberry, T.M.J., Behrenfeld, D.A., Siegel, E., Boss, E. 2008. Carbon-based primary productivity modelling with vertically resolved photoacclimation, *Global Biogeochem. Cycles*, 22, 2024, doi: 10.1029/2007GB003078.

Table 1: Comparison of biogeochemical properties in the Arabian Sea and South Indian Ocean.

Parameter	AS	SIO	t_{stat}
Mixed layer Depth (m)	35.7±8	57.0±15	-4.2; p<0.001
Depth of nitracline (m)	33±5	78±4	-5.6; p<0.001
Photic zone integrated NO ₃ (mmol m ⁻²)	703±220	108±68	6.6; p<0.001
Photic zone integrated PO ₄ (mmol m ⁻²)	70.5±13	47.0±14	5.2; p<0.001
Photic zone integrated Chl- <i>a</i> (mg m ⁻²)	42.5±3	31.6±4	2.8; p<0.01
Photic zone integrated new production (mgC m ⁻² d ⁻¹)	179±86	203±90	-0.1; p>0.8
Photic zone integrated regenerated production (mgC m ⁻² d ⁻¹)	1204±582	1654±263	-3.1; p<0.01
Photic zone integrated net primary production (mgC m ⁻² d ⁻¹)	1238±626	675±431	5.8; p<0.001
Mean <i>f</i> -ratio	0.144±0.06	0.122±0.05	0.2; p>1

Table 2: The photic zone integrated nutrients, *f*-ratio, new (NP), regenerated (RP) and Primary production (PP) in the photic zone of water column.

Stn	LAT	LONG	NO ₃ *	NH ₄ *	ρNO ₃ &	ρNH ₄ &	NP [§]	RP [§]	TP [§]	<i>f</i> -ratio	PP [#]
1	15.43	73.10	1391.7	5.2	13.4	85.6	88.4	564.9	653.3	0.14	228.5
2	15.46	72.03	899.1	34.8	15.7	94.9	103.8	626.3	730.1	0.14	232.7
3	15.45	70.50	620.5	14.9	30.7	128.4	202.6	847.4	1050.0	0.19	272.5
4	15.35	65.00	466.6	11.9	23.8	126.5	157.1	834.9	992.0	0.16	748.9
5	18.17	65.00	847.3	54.5	17.8	106.7	117.5	704.2	821.7	0.14	1367.1
6	21.00	65.00	762.8	41.1	23.3	171.3	153.8	1130.6	1284.4	0.13	1003.2
7	21.88	61.50	981.6	15.7	13.3	174.2	87.8	1149.7	1237.5	0.07	1342.2
8	17.85	61.20	870.8	17.9	16.2	227.8	106.9	1503.5	1610.4	0.07	1557.9
9	15.10	59.80	941.6	23.8	32.3	193.8	213.2	1279.1	1492.3	0.14	1899.9
10	12.90	58.80	394.8	83.2	55.5	406.7	366.3	2684.2	3050.5	0.12	1809.8
11	10.60	58.70	745.9	117.0	23.5	168.4	155.1	1111.4	1266.5	0.12	1687.8
12	8.30	58.63	249.5	43.8	31.8	172.7	209.8	1139.8	1454.8	0.14	1797.6
13	5.60	58.50	406.5	32.2	26.5	175.4	174.9	1160.3	1335.2	0.13	1813.1
14	2.90	58.40	272.3	43.8	40.7	321.8	268.6	2123.9	2392.5	0.11	1572.9
15	-1.00	58.95	307.9	35.1	35.2	209.0	232.3	1379.4	1611.7	0.14	1432.0
16	-5.00	59.35	203.6	16.4	19.9	279.3	197.2	1843.4	1974.7	0.10	792.8
17	-8.10	59.81	101.5	85.9	23.3	192.8	153.8	1272.5	1426.3	0.11	893.5
18	-27.95	63.54	28.6	58.9	33.3	292.6	219.8	1931.2	2151.6	0.10	770.1
19	-27.85	64.02	2.3	79.8	20.9	228.6	137.9	1508.8	1646.7	0.08	236.1
20	-26.92	66.83	22.3	27.8	28.8	268.8	190.1	1774.1	2162.2	0.10	331.4
21	-26.33	67.91	17.9	84.7	24.2	283.1	159.7	1868.5	2028.2	0.08	269.0

* photic zone integrated concentrations (mmol m⁻²)

NP=New Production; RP=Regenerated Production and TP=Total production

§ Photic zone integrated production rates (mgC m⁻² d⁻¹)

#Photic zone integrated Net primary production (mgC m⁻² d⁻¹)

&ρNO₃ and ρNH₄ are photic zone integrated nitrate and ammonium uptake rates (mgN m⁻² d⁻¹)

Legend to figures:

Figure 1: Study area depicting station locations overlaid on mean a) Sea surface temperature ($^{\circ}\text{C}$), b) Sea surface salinity, c) Sea surface Chlorophyll-*a* (mg m^{-3}) and d) sea surface height anomaly (m) (color shading) and geostrophic currents (m/s) (arrows) during September 2015.

Figure 2: Depth-distance sections of a) temperature ($^{\circ}\text{C}$), b) salinity (psu), c) Chlorophyll-*a* (mg m^{-3}) and d) dissolved oxygen (μM) in the upper 100m along the cruise track. The sampling depths are shown as black dots. The station numbers are given in the upper axis. White block represents the region where no data collected.

Figure 3: Depth-distance sections of a) dissolved nitrate (μM), b) ammonium (μM), c) dissolved phosphate (μM) and d) dissolved silicate (μM) in the upper 100m along the cruise track. The sampling depths are shown as black dots. The station numbers are given in the upper axis.

Figure 4: Photic zone integrated a) new production, b) regenerated production, c) primary production (all in $\text{mgC m}^{-2} \text{d}^{-1}$) and d) *f*-ratios in the sampling stations. The station numbers are also shown.

Figure 5: Relationship of photic zone integrated Chl-*a* with photic zone integrated primary production. Note that coastal stations (1-3) were not considered in this relationship.

Figure 6: Relationship of photic zone integrated primary, new, regenerated productions and *f*-ratios with depth of nitracline (a-d), primary production with e) mixed layer mean temperature and f) N/P ratio, *f*-ratio with f) mixed layer mean temperature and h) photic zone integrated Chl-*a* (mg m^{-2}).

Figure 7: The relationship of photic zone integrated new, regenerated and primary productions with photic zone integrated nitrate (a-c) and phosphate (d-f) in the study region.

Figure 8: a) Comparison primary production by CbPM (blue line), VGPM (red line) with measurements (black line) and b) the percentage of deviation of primary production by models from that of observations. Coastal stations (stn. 1-3) were not considered.

Figure 1

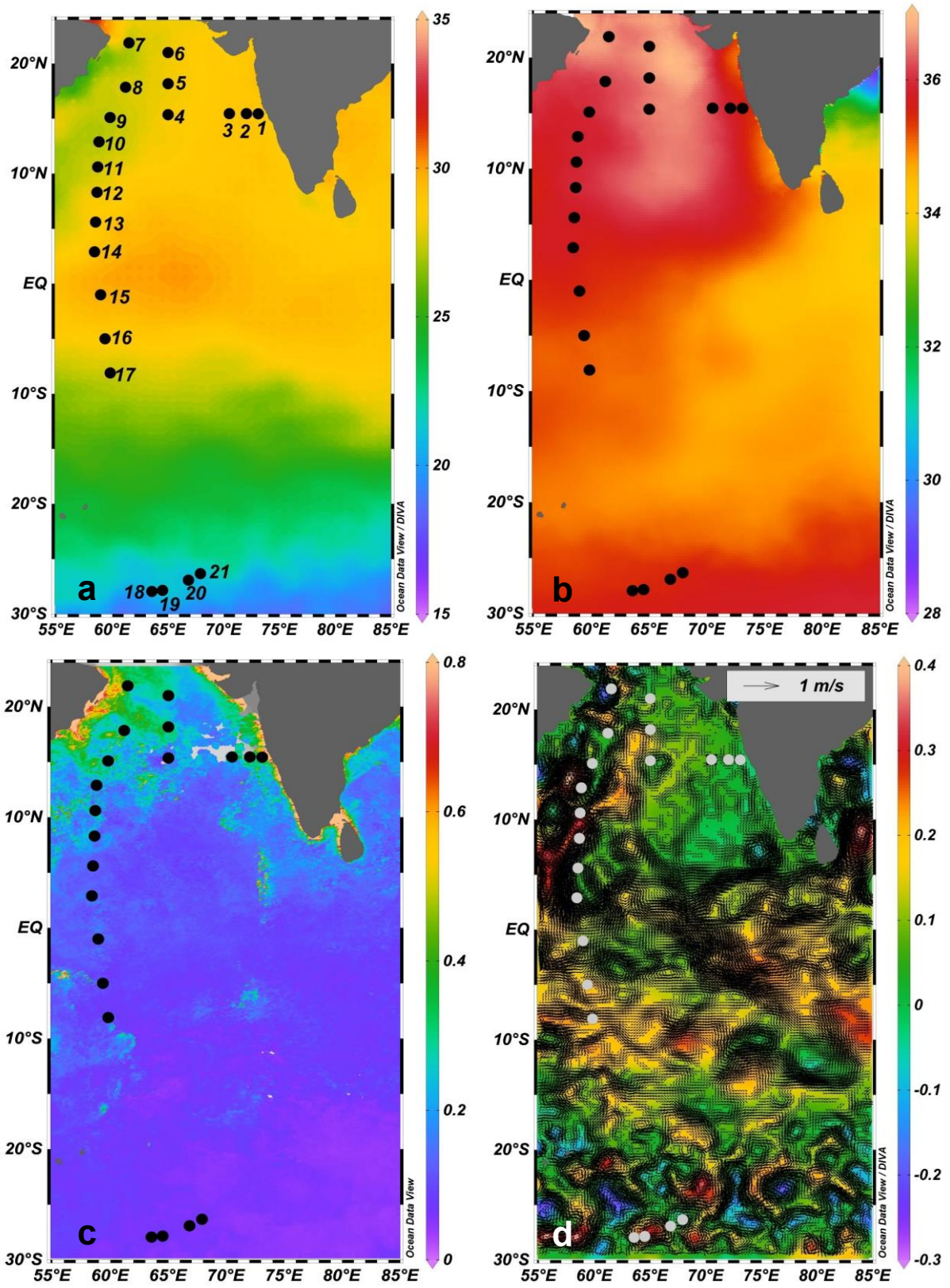


Figure 2

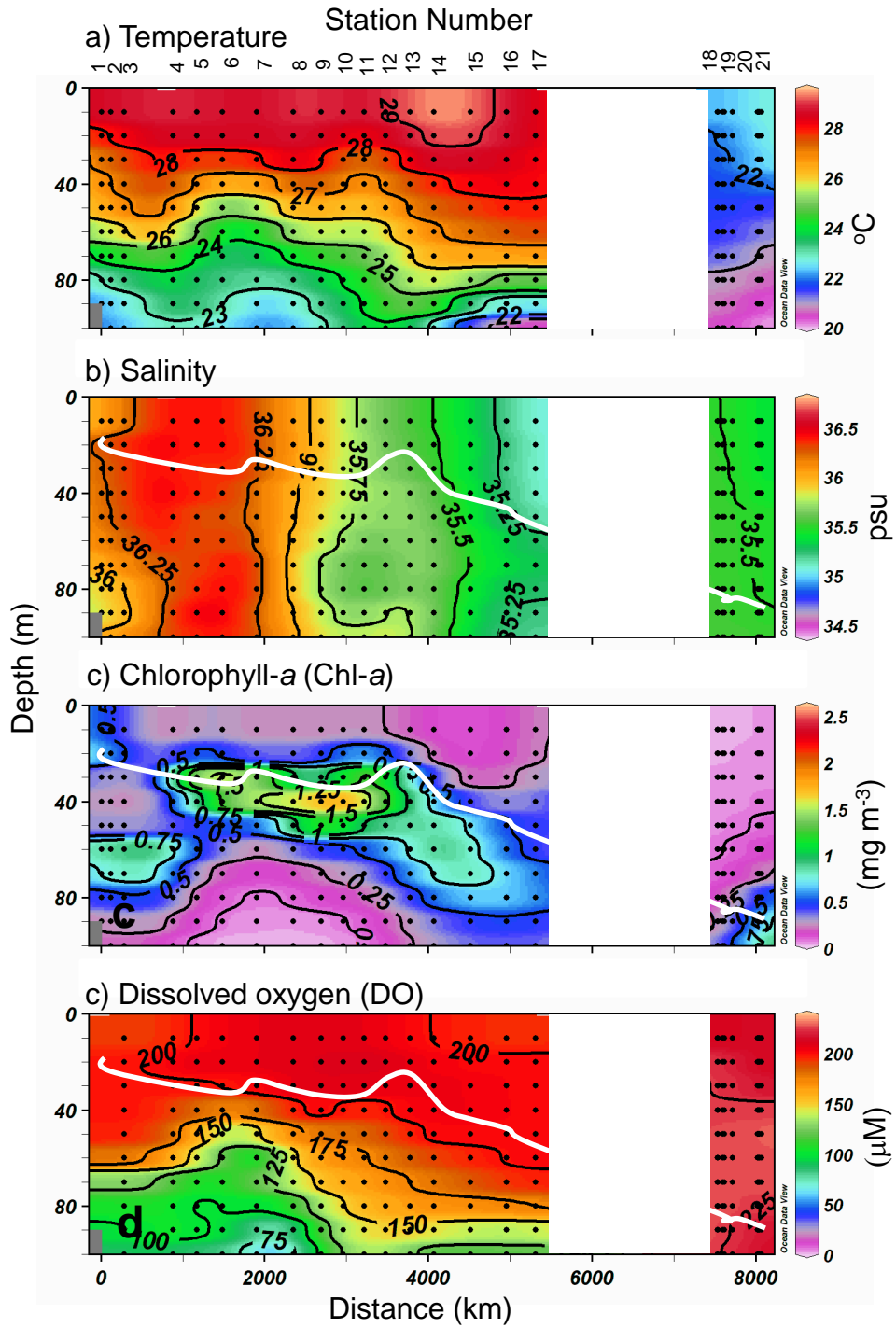


Figure 3

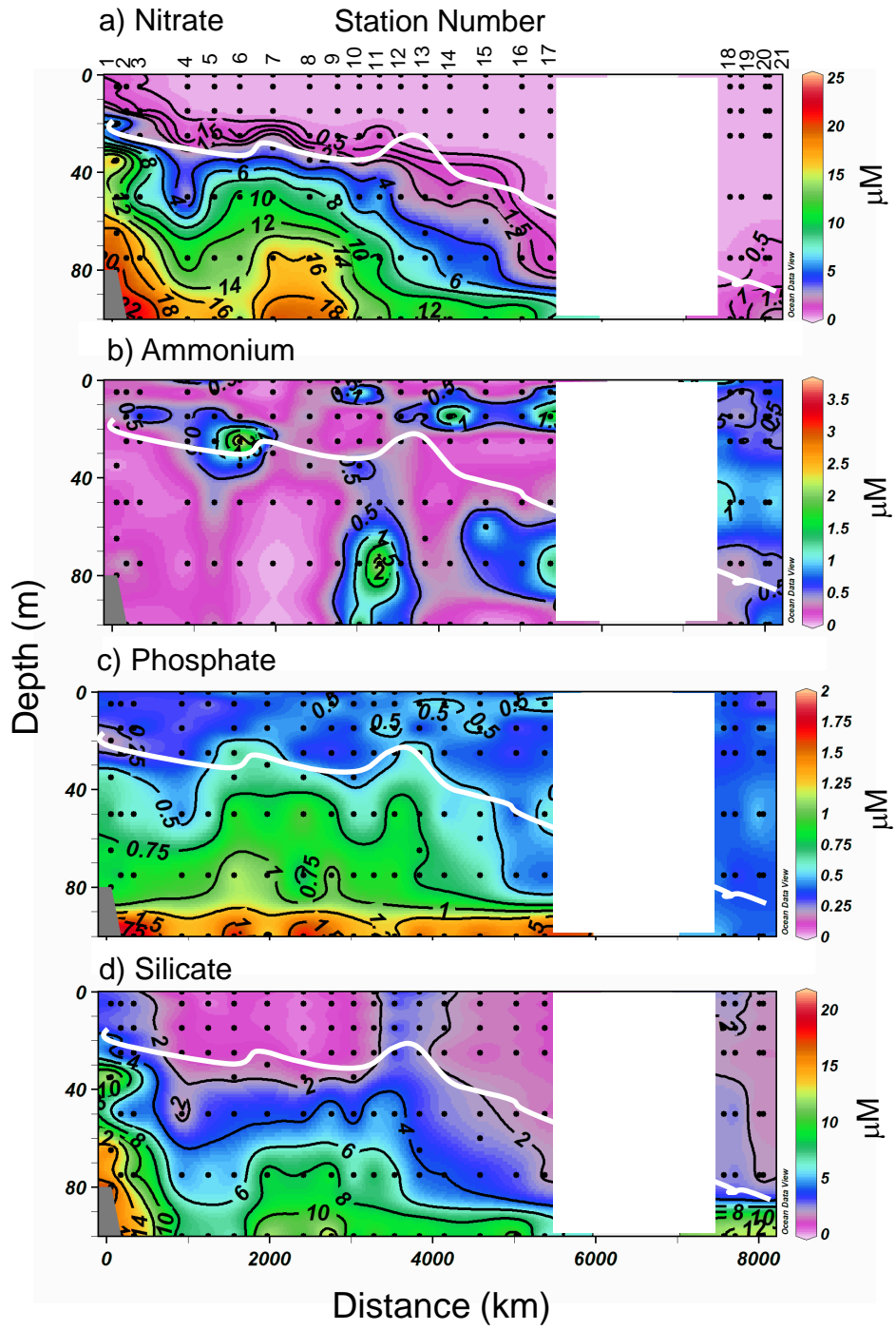


Figure 4

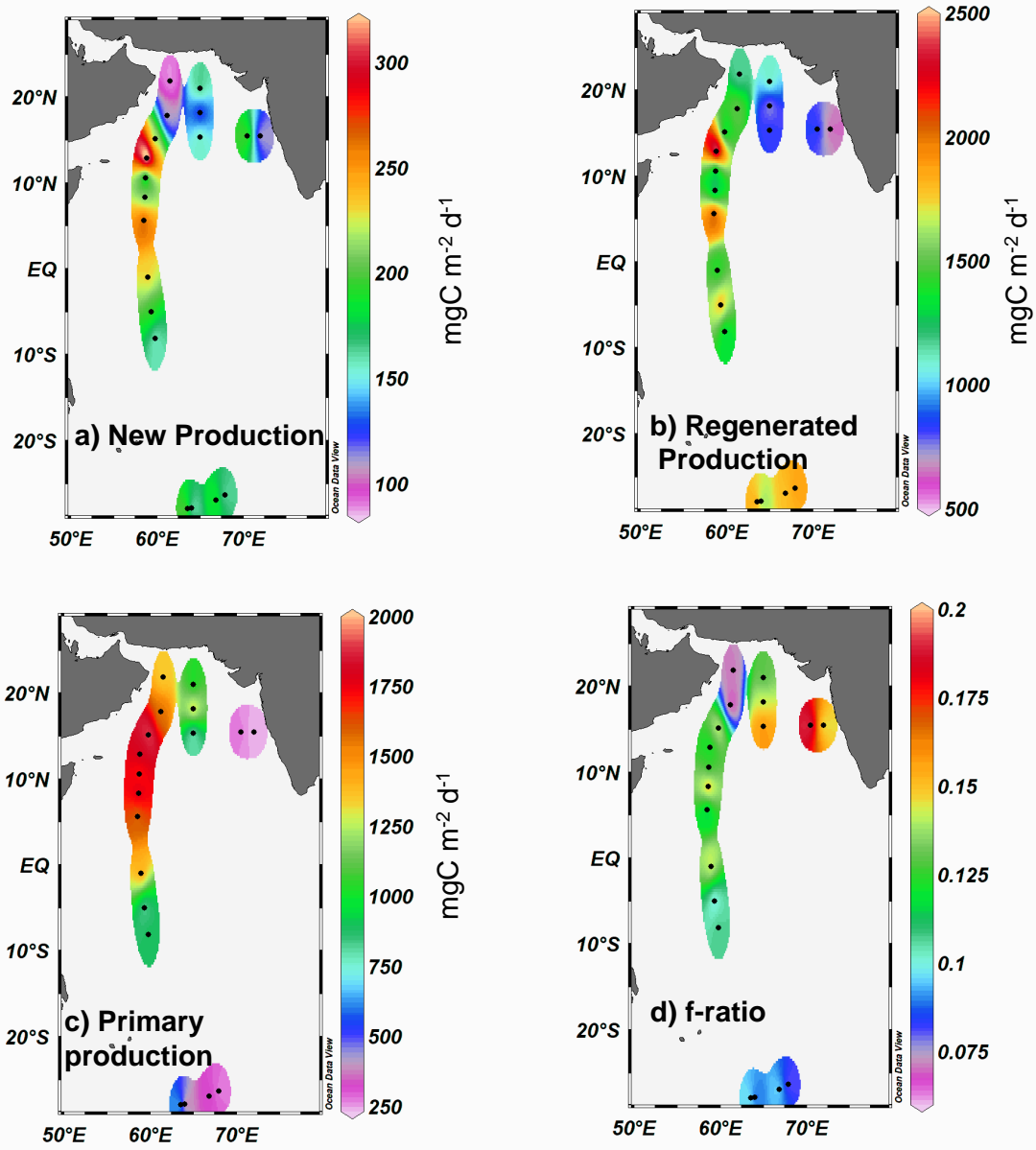


Figure 5

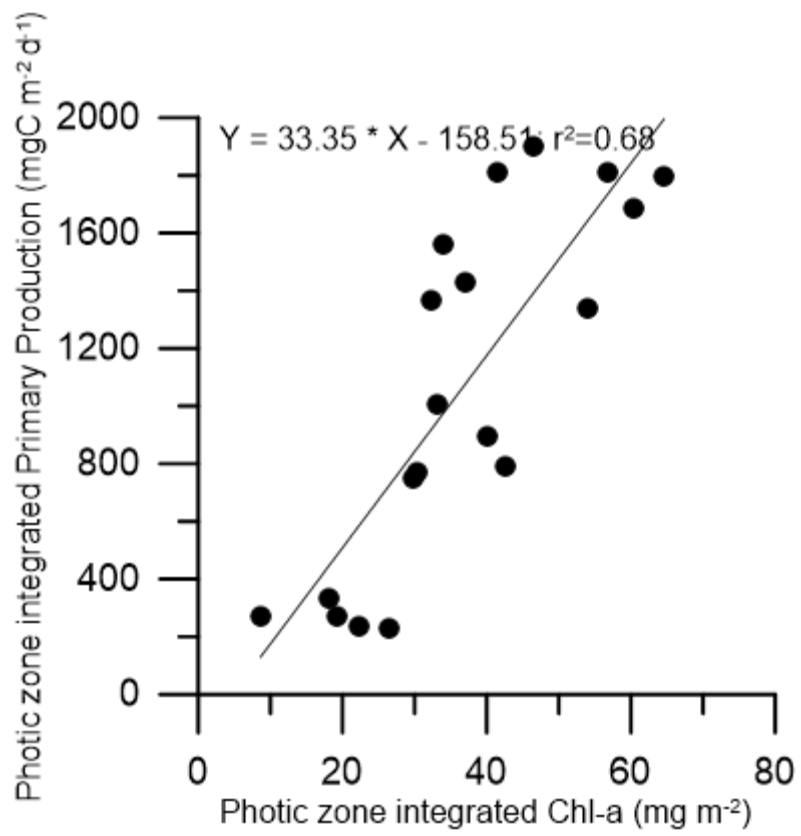


Figure 6

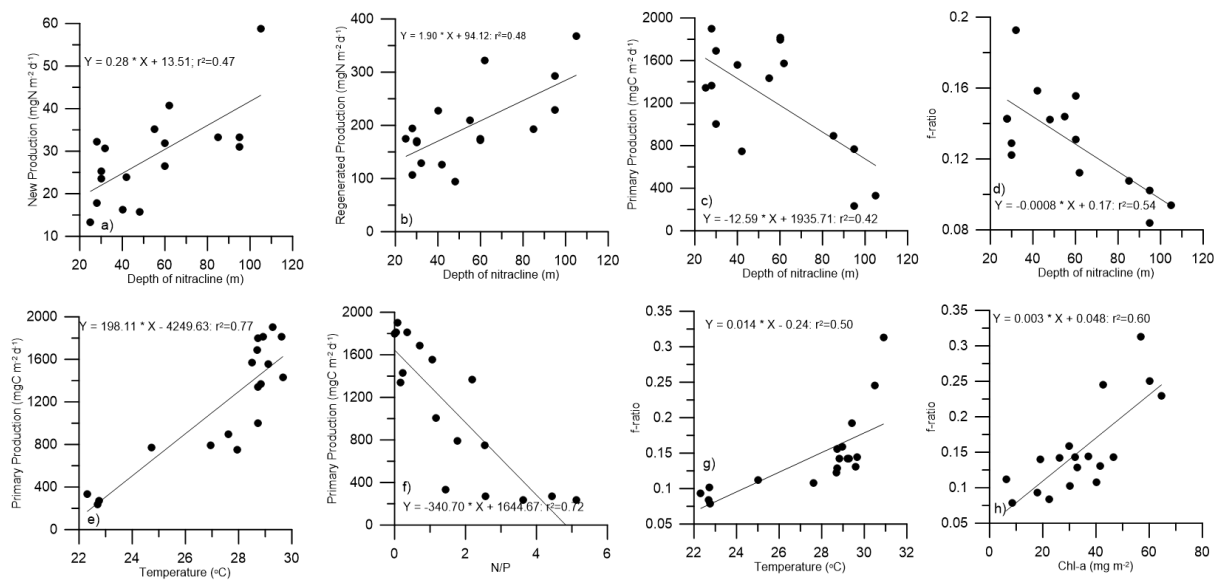


Figure 7

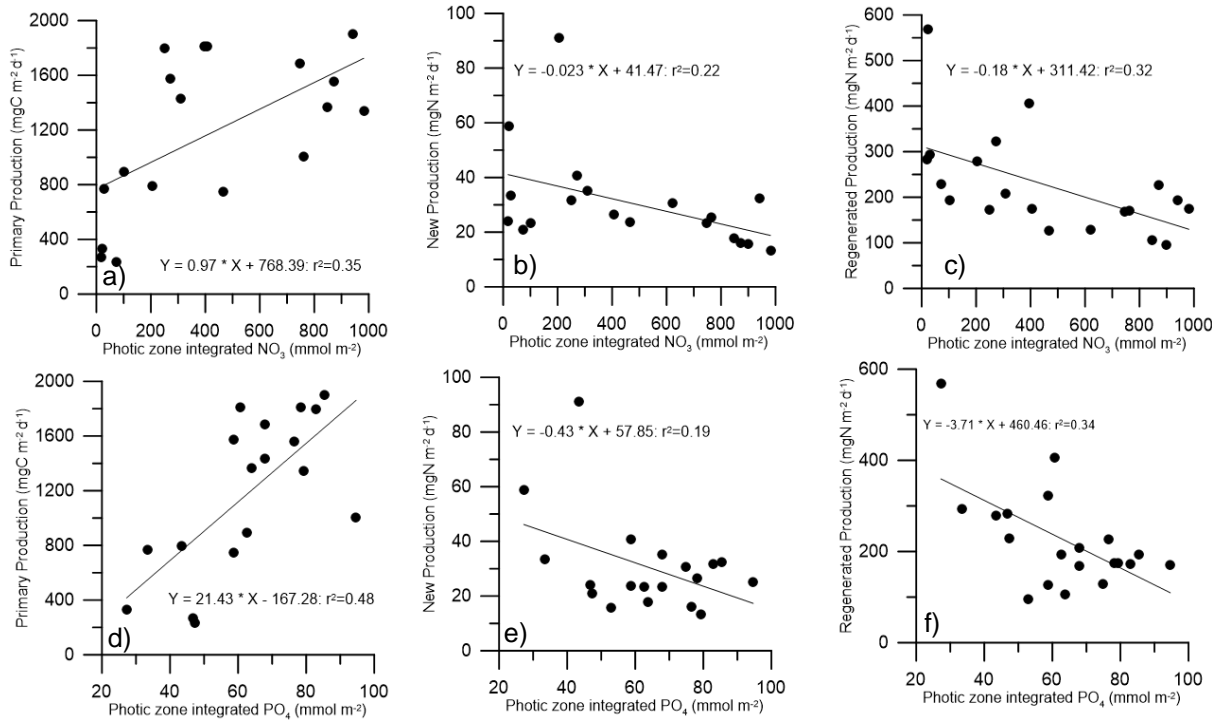
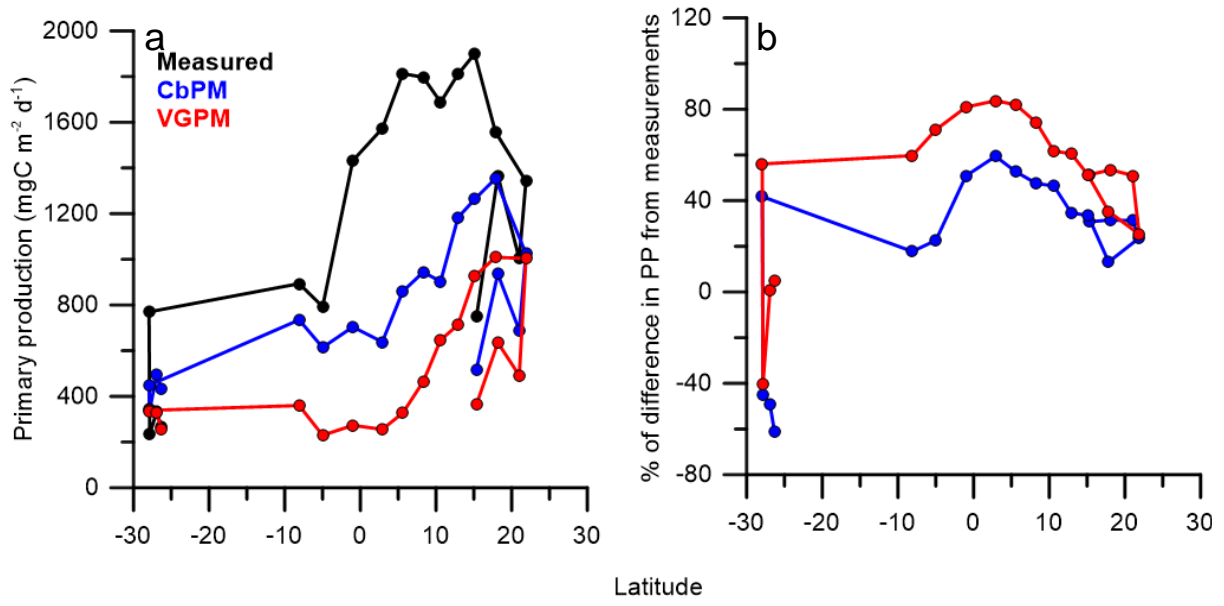


Figure 8



Supplementary Figure S1: The SSHA (color scale) and surface currents directions (arrows) on the day of collection. The white dots and number indicates station location and its number (as per Figure 1) are also shown.

